Validating Quantitative Micro-Ultrasound Method for Monitoring the Development of Liver Steatosis in Mouse Model

David Chibuike Ekwe

Master's thesis

University of Turku
Faculty of Medicine
23.04.2024

Master's degree in Biomedical Imaging
Specialization theme: Medical Imaging

Credits: 40 ECTS

Supervisors:

Adj. Prof. Leena Strauss

Hanna Heikela (PhD)

Laura Mairinoja (MSc)

Endocrine Signaling Consortium
Institute of Biomedicine
University of Turku

Abstract

UNIVERSITY OF TURKU
Faculty of Medicine
Institute of Biomedicine

DAVID CHIBUIKE EKWE:

Validating quantitative micro-ultrasound method for monitoring the development of liver steatosis in mouse model

Master's thesis, 41 pp.
MSc in Biomedical Imaging
04 2024

Non-alcoholic fatty liver disease (NAFLD) is a condition where the liver accumulates fat without the influence of alcohol. The exact cause of NAFLD is not well understood but it is linked to a syndrome of metabolic disorders that influence and significantly alter how the body metabolizes and stores fat. Given that NAFLD is a progressive disease, longitudinal *in vivo* studies are needed to track and understand how the disease evolves and how the preclinical models respond to therapeutic interventions. While liver biopsy and histologic analysis remain the gold standard for the diagnosis of NAFLD, its invasiveness and high sampling variability make it impractical for the serial assessments in longitudinal preclinical studies. Micro-ultrasound, a non-invasive imaging technique for research animals, is a promising technique for conducting longitudinal studies of NAFLD models. However, the level of accuracy of this technique is not confirmed. The objective of this study was to establish the validity of a reliable and reproducible method of detecting the presence of hepatic steatosis in mice using quantitative ultrasound technique. Ten mice on high fat diet (HFD) and ten on chow were studied for 12 weeks and five mice from each group were assessed using micro-ultrasound. B-mode images of the liver were acquired and used to calculate the hepatic-renal ratio (H/R). This parameter was correlated with the biomarkers of hepatic steatosis for validation. The HFD mice developed hepatic steatosis as evidenced by the increased lipid droplets in histologic analysis, higher serum ALT activity, increased liver triglyceride concentration and body fat composition. Quantitative ultrasound was able to reliably differentiate between fatty liver and healthy controls (fold change 2.36, $p<0.001$) in a manner that corresponds to the indications of other biomarkers of hepatic steatosis. The H/R ratio had a positive correlation with the body fat, liver triglyceride content, serum ALT and histological image analysis ($R = 0.62, 0.46, 0.92, 0.88$, respectively). The results of this study indicate that quantitative micro-ultrasound technique is a feasible non-invasive approach for longitudinal evaluation of intra hepatic fat in preclinical mouse models.

KEYWORDS: NAFLD, Quantitative ultrasound, Hepatic-Renal ratio, mice, Hepatic steatosis, Image analysis, longitudinal study

List of abbreviations

ALT	Alanine aminotransferase
DL	Deep Learning
FC	Fold change
H & E	Haematoxylin and Eosin
H/R	Hepatic - renal ratio
HFD	High fat diet
HSD17β13	hydroxysteroid 17-beta dehydrogenase 13
NAFLD	Non-alcoholic fatty liver disease
NASH	Non-alcoholic steatohepatitis
ROI	Region of interest
WSI	whole slide images

Index

INTRODUCTION

1.1 Non-Alcoholic Fatty Liver Disease (NAFLD)

NAFLD is a liver condition characterised by the accumulation of fat in the liver (hepatic steatosis) independent of alcohol abuse. It describes a continuum of liver pathology with varying degree of severity, beginning with aberrant accumulation of fat in the liver (exceeding 5% by weight) which may progress to non-alcoholic steato-hepatitis (NASH) where the accumulation of fat in the liver is accompanied with inflammation and hepatocellular damage. Overtime, NASH may evolve to fibrosis and potentially culminate in hepatocellular carcinoma (Haas et al., 2016) (figure 1). Currently, the global incidence of NAFLD is on the rise, mirroring the upward trend in other lifestyle-related conditions, such as diabetes and obesity, resulting in the heightened risk of liver-related fatalities among the populace (Samji et al., 2019). Approximately 32% of the adult population is estimated to be affected by NAFLD with the prevalence in men nearly two times higher than in women, making it the leading indication for hepatocellular carcinoma and liver transplantation (Teng et al., 2023).

The exact cause of NAFLD is not completely understood, but it is strongly associated with such metabolic disorders as diabetes, obesity, dyslipidemia and hypertension (Chalasani et al., 2018). Systemic insulin resistance significantly contributes to the development of NAFLD by disrupting the normal regulation of fatty acids in the body, leading to the excess delivery of fatty acids to the liver beyond the liver's capacity to metabolize them (Friedman et al., 2018). It has also been reported that damage to the intestinal tight junctions due to increased endogenous production of ethanol by intestinal microflora, may contribute to the development and progression of NAFLD (Robinson & Shah, 2020). Furthermore, genetic variations in hepatic lipid metabolism play a role in making an individual susceptible to the disease. The dynamic interplay between this genetic susceptibility and environmental factors are critical in determining the disease phenotype and progression (Eslam et al., 2018). Thus, the clinical manifestation and the disease progression is highly variable among individuals as the pathogenic drivers are likely different for each individual (Friedman et al., 2018).

As a result of the heterogenous nature of the disease, there is currently no well-established treatment for NAFLD beyond lifestyle changes involving diet and exercise, highlighting the need for further research on the disease (Cohen et al., 2011). It has been suggested that early detection and inhibition of hepatic steatosis may prevent the progression of NAFLD to lethal stages, as previous studies have shown that nearly 1/3rd of NAFLD cases may progress to irreversible liver damage within 10 years (Argo & Caldwell, 2009; Hernaez et al., 2011a). However, our ability to identify those at high risk of disease progression is hampered by the lack of sufficient longitudinal data, the absence of reliable biomarkers for the different stages of the disease and the significant heterogeneity of the disease phenotype (Cohen et al., 2011; Bence & Birnbaum, 2020). These complexities have necessitated the use of preclinical models to unravel the pathogenesis of the disease, the molecular mechanism of progression and to develop therapeutic interventions (Flessa et al., 2022).

Histopathological analysis, though an invaluable technique in preclinical research, is not suitable for longitudinal studies of preclinical models as it necessitates euthanizing the animals at different time points (Rowles et al., 2019). This limits the ability to track the responses of individual animals over time and to assess the variability within the group. Furthermore, it hinders the complete understanding of the disease development as the dynamic changes that may occur between time points such as the rate of progression or potential reversibility of observed changes are not captured. Thus, alternative non-invasive techniques that can be used to reliably monitor the development of NAFLD over time and assess the response to therapeutic interventions in preclinical models are needed.

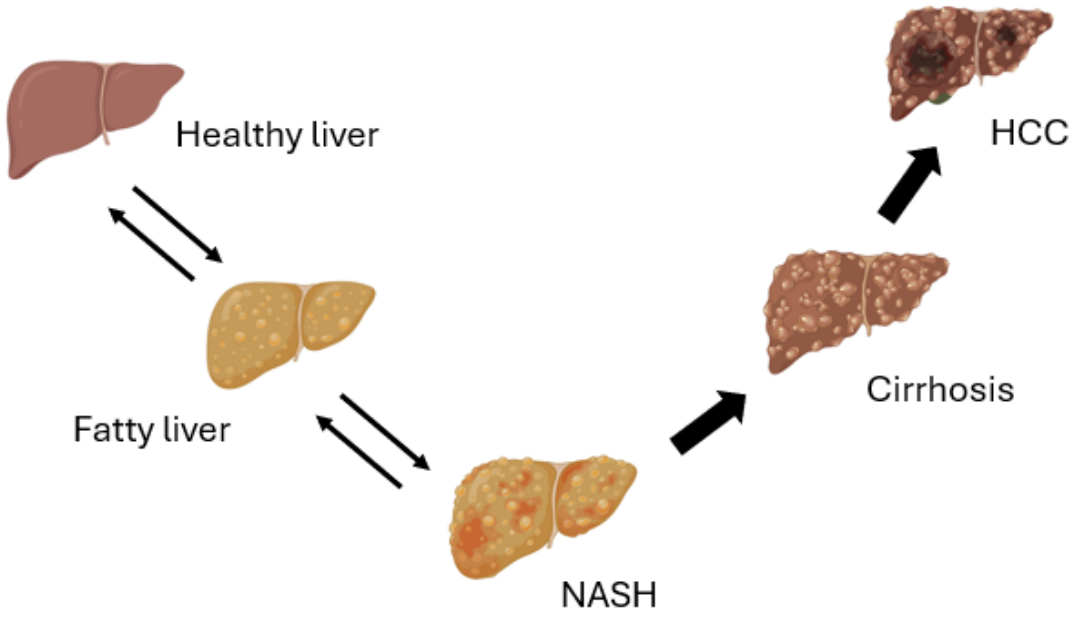

Figure 1: Diagrammatic representation of the different stages of NAFLD progression.

1.2 Animal Models of NAFLD

Animal models of NAFLD are invaluable for understanding the development of NAFLD and for evaluating the effectiveness of different treatments, given that it circumvents the ethical limitations associated with obtaining human samples for research or recruiting NAFLD patients for studies (Van Herck et al., 2017). A number of NAFLD animal models – chiefly mice and rats – have been developed to study the disease progression and guide therapeutic interventions, and these can be broadly grouped into diet – induced models, genetic models and a combination of both models (Takahashi et al., 2012).

1.2.1 Genetic Models

The genetic mouse models have mutations that precipitate the spontaneous development of NAFLD (Flessa et al., 2022). The mutations in the genetic mouse model can be either

spontaneous or genetically modified. Examples of spontaneous models are, *ob/ob* mice, which are deficient in leptin – a hormone that plays a role in regulating appetite and metabolism, leading to hyperphagia, obesity, hyperglycemia, and insulin resistance, and *db/db* mice, which have a nonfunctional leptin receptor and exhibits a similar phenotype to *ob/ob* mice (Jacobs et al., 2016).

There are several genetically modified mouse models, which can be used to study NAFLD. For example, the knockout of hydroxysteroid 17-beta dehydrogenase 13 enzyme (HSD17β13) has been demonstrated to induce severe hepatic steatosis and inflammation in adult mice. With age, the HSD17β13KO mouse model developed steatosis but without the characteristic metabolic syndrome of obesity and insulin resistance (Adam et al., 2018a).

Conversely, *foz/foz* mouse model has a mutation in *Alms1* gene, which encodes a protein believed to be involved in appetite regulation and intracellular transport. The mice are hyperphagic and develop the metabolic complications of NAFLD including morbid obesity, insulin resistance and hepatic steatosis. Interestingly, depending on the strain of the *foz/foz* mice, feeding them with high fat diet exacerbates their metabolic complications and induces the progression into NASH with severe fibrosis (Bell-Anderson et al., 2011; Lau et al., 2017).

Overall, these and other genetic models are important for studying the different aspects of the diseases as they simulate the pathological characteristics of the disease to a certain extent. However, each model exhibits distinct limitation in capturing the full range of the NAFLD spectrum. Thus more animal models that closely mirror the complete disease spectrum are needed to elucidate the pathogenesis and progression of NAFLD and to identify potential therapeutic targets (Jacobs et al., 2016; Lau et al., 2017).

1.2.2 Diet-Induced Models

Diet – induced models closely mimic the processes, patterns and chronological sequence of events that occur in the pathogenesis of NAFLD in human, making them suitable models to study the initial liver damages that trigger the onset of NAFLD (Stephenson et al., 2018). They predominantly involve the use of either single or a combination of dietary regimens

including high-fat, high-fructose, cholesterol and cholate, methionine and choline deficient diet, among others, to induce simple steatosis and steatohepatitis (Zhong et al., 2020).

High-fat diet is a dietary regimen in which fat makes up 45-75% of the total calories. It is a common choice for making animal model of NAFLD, as animals fed with HFD for 3 weeks are reported to develop hepatic steatosis characterized by increased liver triglyceride levels and insulin resistance with elevated plasma insulin level. (Lau et al., 2017; Zhong et al., 2020). Thus, HFD animals mirror key aspects of NAFLD in humans, although the extent of liver fat accumulation appears to vary with rodent strain and other factors (Zhong et al., 2020).

Western diet is characterized by high levels of saturated fat, sucrose, fructose and low fiber content. It has been reported that western diet intake induces obesity, hepatic steatosis, inflammation and fibrosis in mice, replicating the characteristic pathological features of non-alcoholic steatohepatitis. The interplay between western diet and the gut microbiota is said to produce the metabolites that are implicated in the onset and progression of NAFLD (Abu-Shanab & Quigley, 2010; Yang et al., 2023).

Methionine and choline deficient (MCD) diet is a well characterized dietary model consisting of high sucrose and moderate fat content but lacking in methionine and choline – essential nutrients for hepatic functions (Lau et al., 2017). Choline deficiency in this diet impairs the livers ability to secrete very-low-density-lipoprotein (VLDL), leading to an accumulation of lipid in the liver, oxidative stress and hepatocellular death (Ibrahim et al., 2016). It replicates the histological features seen in human NAFLD and steatohepatitis in a relatively short feeding time, but lacks the corresponding metabolic features such as obesity, peripheral insulin resistance and dyslipidemia. MCD diet is a typical dietary intervention for inducing hepatic inflammation and fibrosis (Van Herck et al., 2017; Sahai et al., 2004).

1.3 Micro-ultrasound Imaging and Digital Pathology to Study Mouse Liver Steatosis

Micro-ultrasound is a valuable *in vivo* technique for assessing liver fat content and other metabolic disorders in mouse models, given that it is non-invasive, non-ionizing, widely available and can be used to perform longitudinal studies which enables the characterization of disease progression (Di Lascio, Kusmic, et al., 2018). The diagnosis of liver steatosis using ultrasound is based on the premise that elevation in liver fat content induces several observable changes in the ultrasound image (Figure 2). The changes encompass increased echogenicity of the liver tissue relative to surrounding structures and poor visualization of intrahepatic structures due to the attenuation of ultrasound beam (Di Lascio, Avigo, et al., 2018). The drawback to this technique is that it relies on the subjective assessment of the operator rather than on precise measurements, making the results more open to interpretation (Hannah Jr. & Harrison, 2016). It is also reported to be limited in its ability to accurately detect and distinguish mild cases of steatosis (Martín-Rodríguez et al., 2014). However, it has been suggested that accurate and reproducible assessment of liver steatosis can be carried out through quantitative analysis of the fat-induced alteration in liver ultrasound images (Di Lascio, Avigo, et al., 2018). One approach to derive quantitative data from ultrasound image is through the use of image analysis techniques like pixel intensity distribution (Wu et al., 2016). In order to validate an *in vivo* technique in preclinical research, it is imperative and often a prerequisite to correlate the result of the technique with those of established ex vivo methods like histological analysis (Stockinger et al., 2021).

The advent of digital pathology has opened up new possibilities for the examination of tissue samples and the extraction of information from digital image data in more efficient and versatile ways compared to traditional glass slides and microscopy techniques (Barisoni et al., 2020). The digitization of tissue samples into whole slide images has paved the way for the integration of computer-aided quantitative tools for image analysis which ensures improved objectivity and consistency in the quantification and measurement of specific tissue feature during research. It also enables the deployment of artificial intelligence and machine learning models for deeper insights into tissue characteristics and

automation of repetitive tasks (Jahn et al., 2020; Chen et al., 2022; Kiran et al., 2023). Furthermore, digital pathology significantly enhances productivity in research by facilitating extensive collaboration through easy remote access to, and central storage of digital slides (Kiran et al., 2023). The implementation of digital pathology in research requires a substantial initial investment in computer hardware, software and robust data management and storage solutions. However, in the long term, it offers significant benefits that far outweighs the initial costs in terms of enhanced productivity, improved analysis and interpretation of tissue characteristics, standardization of protocols to enhance reproducibility and reliability of research findings, which facilitates innovation (Ho et al., 2014).

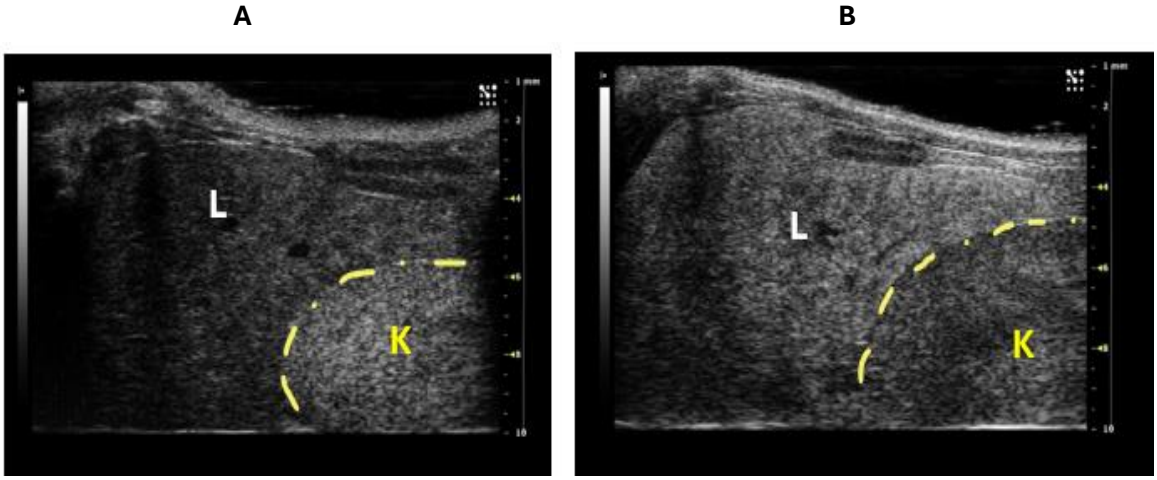

Figure 2: Micro-ultrasound B mode image of (A) mouse liver that is normal and (B) mouse liver with hepatic steatosis. The difference in the echogenicity of the median lobe of the liver (L) with respect to the right kidney (K) in each of the image is the basis for the subjective assessment of steatosis.

This study validates the quantitative micro-ultrasound technique for *in vivo* longitudinal assessment of liver steatosis in diet-induced mouse models. Validation employed the comparison of the technique with established biomarkers of NAFLD including body fat composition, serum ALT levels, liver triglyceride level and deep learning-based image analysis of liver histological sections. Given that there are currently no widely used biomarkers in preclinical research for monitoring the development of liver steatosis *in vivo*,

this technique not only provides a useful framework for evaluating lipid accumulation in the liver at different time points, but also advances the 3R principle (Replacement, Refinement and Reduction) of scientific research by reducing the total number of animals in the future studies.

2. AIMS AND HYPOTHESIS

We hypothesized that quantitative micro-ultrasound imaging can be used to follow the development of fatty liver disease in mice. The following were the aims of the study:

1. To determine the feasibility of monitoring the development of hepatic steatosis in mice over time using micro-ultrasound imaging.

2. To ascertain if this method is sensitive enough to detect the differences between the groups.

3. To evaluate the quantitative accuracy of micro-ultrasound technique by correlating it with other markers of fatty liver disease like body fat composition, serum ALT, liver triglyceride concentration, liver weight and deep learning-based image analysis of liver histology.

3. MATERIALS AND METHODS

3.1 Animals

All animal work was conducted at the Turku Center for Disease Modelling, University of Turku (Turku, Finland) under the animal licence number ESAVI/23322/2023 granted by the Animal Experiment Board in Finland. Animal handling was performed in accordance with the institutional animal care policies that fully meet the requirements as defined in the NIH guidelines on animal experimentation.

Twenty C57BL/6 male mice were used in this experiment. The animals were singly housed in individually ventilated cages (Techniplast, Buguggiate, Italy) with approximately 70 air changes per hour. Constant temperature (21°C ± 3°C) and humidity (55% ± 15%) were maintained together with a consistent 12-hour light – dark cycle, with a light change at 7 am and 7 pm. Autoclaved aspen chips were used as bedding (Tapvei Ltd, Harjumaa, Estonia). Manila software (https://ensigcon.shinyapps.io/rvivo/) was used to randomly divide the mice into 2 groups of 10 mice each for the diet intervention. Group 1 mice were fed normal chow (Teklad rodent diet, Inotiv, Wisconsin, USA) Group 2 mice were fed high fat diet (HFD), (D17010103, Research Diets, Inc. New Brunswick, USA). The chow pellet, HFD pellet and autoclaved tap water from the public supply (Turun vesilaitos, Turku, Finland) were provided for the animals *ad libitum*. The diet intervention lasted for 12 weeks and during this period, the weights of the animals were measured weekly, ultrasound and echoMRI studies were carried out monthly and blood samples were taken fortnightly. At the end of the experiment, the mice were euthanized by CO_2 asphyxiation and cervical dislocation. The kidneys and gonadal fat pads were excised for measurement and liver tissues were also taken for histology and triglyceride measurement.

3.2 Body weight, Body composition and Tissue weight

The body weight of the mice was measured and recorded once every week using a weighing scale PG2002 (Mettler Toledo, Greifensee, Switzerland). Each mouse, identified by their cage number was gently picked up from its cage and placed in the cardboard box placed on the calibrated weighing scale. The weight was recorded as soon as the reading on the scale stabilized, and the mouse was gently returned to its cage.

The body composition was measured once every month using the EchoMRI-700TM device (Echo Medical Systems, Houston, USA). After setting up the machine, each mouse was gently guided into the clear tube-like plastic holder that have openings for ventilation. The second component of the plastic holder was then used to gently and securely immobilize the mouse in a comfortable position. The holder was then inserted into the tubular space within the EchoMRI machine, and the scanning began. Each scan lasted for less than 3 minutes, after which the mouse was immediately returned to its cage.

At the end of 12 weeks, the animals were euthanized. The liver, kidneys and gonadal fat pads were taken from all the animals and weighed on the scale AG204 (Mettler Toledo, Greifensee, Switzerland) and thereafter, stored in liquid nitrogen and formalin.

3.3 Blood Sampling

Blood sample for determination of serum ALT level were collected from the lateral saphenous vein of each of the 20 mice without anaesthesia. The mice were immobilized using a 50 ml falcon tube with opening for ventilation. The hair on the rear lateral portion of the leg were shaved and the skin dabbed with alcohol wipe. Digital pressure was applied from behind the knee to help visualize the saphenous vein. The blood vessel was then punctured with sterile 25G needle, and the blood sample (100 µl) was collected into labelled serum separation tube (BD Microtainer, Becton Dickinson, Franklin Lakes, USA) using glass capillary. After 30minutes, the samples were centrifuged at 10,000 rpm for 2minutes to separate the serum. The serum was then transferred into a labelled 1.5 ml Eppendorf tube using a pipette tip and stored in -80°C freezer. Serum ALT level was measured from these samples by Movet Oy, in Kuopio, Finland, using the Konelab 60i Chemistry analyzer (Thermo Fisher Scientific, Massachusetts, USA).

3.4 Micro-ultrasound Examination

Five mice from each group were randomly selected for micro-ultrasound studies. The mice were prepared for the examination by anaesthetizing the animal with isoflurane (3% isoflurane in 1L/min of oxygen) in an induction chamber connected with a scavenger cannister. After induction, the mouse was placed on its back on a temperature-controlled board at 36°C, with its limbs stretched out and secured in a way that minimized motion during the scan. A nose cone was used to maintain the mouse under gaseous anaesthesia (1.5% isoflurane) during the procedure. The abdominal hair was then shaved off using animal hair clipper and depilatory cream, then warm acoustic coupling gel, Eco Supergel (Ceracarta, Forlì, Italy) was generously applied on the abdomen and the 40MHz probe (MX550D) of the high-frequency micro-ultrasound imaging device (Vevo 2100, VisualSonics Inc., Toronto, Canada), held in position by a mechanical arm, was used for

image acquisition (Figure 3). The acquired image was an Ultrasound B-mode scan of the liver acquired from a longitudinal projection that have both the medial lobe and right kidney of the mice in the same image and both organs at the same depth.

3.5 Histological Analysis

Tissue samples from right kidney and the medial lobe of the liver were collected from all the animals for histological analysis. The samples were fixed in 10% formalin at room temperature for 24 hours, dehydrated in ascending series of alcohol, cleared with xylene and embedded in paraffin wax. The embedded tissues were cut into thin sections (4 µm) with a microtome, mounted on a glass slide and stained with Haematoxylin and Eosin (H & E) following the standard procedures.

Figure 3: Image of the micro-ultrasound device and its accessory components including the induction chamber, temperature-controlled board, mechanical arm, and movable stage.

3.6 Deep Learning-based Image Analysis

Tissue slides of the liver prepared by histological technique and stained with H & E, were scanned with Panoramic 1000 Flash digital slide scanners (3DHISTECH Ltd, Budapest, Hungary) with ×20 magnification with a resolution of 0.24 μm/pixel, to generate whole slide images (WSI) . The WSIs of the liver were converted to a readable format for the software and uploaded to the Aiforia Create cloud platform. Hepatic steatosis was quantified from the WSIs of H & E-stained liver samples using the deep learning model created on Aiforia Create (version 6.0, Aiforia technologies, Helsinki, Finland). The model detects and quantifies micro- and macrovesicular steatosis within the liver parenchyma, but excludes background, artefacts and blood vessels (Mairinoja et al., 2023) (Figure 4).

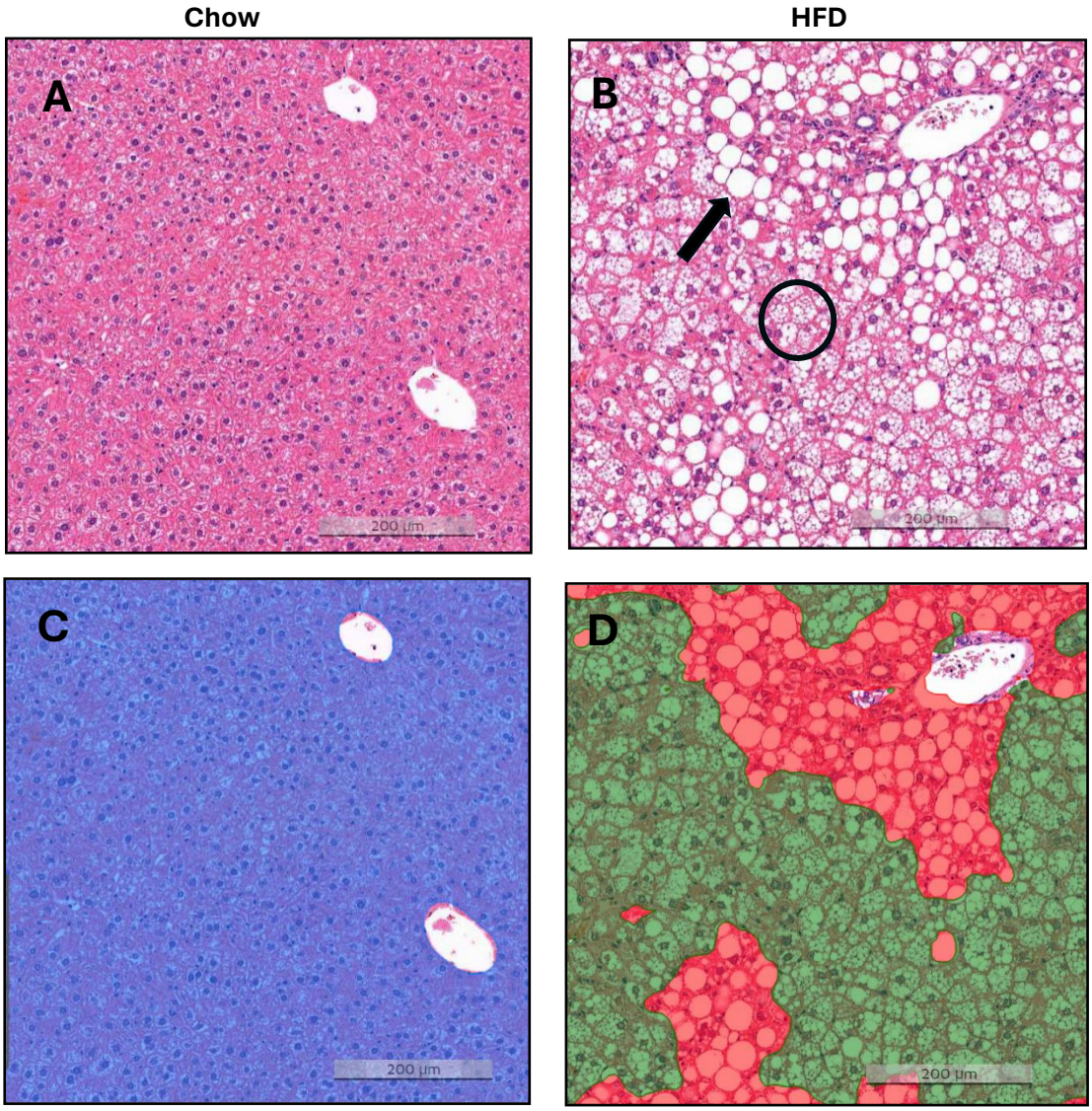

Figure 4: Histological images of haematoxylin & eosin-stained liver tissues showing **(A)** homogeneous parenchyma with normal hepatocytes in chow mice **(B):** macrovesicular lipid droplets **(arrow)** and microvesicular lipid droplets **(circle)** in HFD mice. **(C)** The model detects the liver parenchyma and excludes blood vessels and fixation artefacts. **(D)**The

3.7 Triglyceride measurement

To measure liver triglyceride content, about 100mg was cut from frozen liver sample. The cut piece was weighed in a contamination – free scale and allowed to thaw on ice. It was then homogenized in 500 µl of ice-cold 0.1% Trixton X-100 in Phosphate buffered saline (PBS) with Tissue Lyser (Qiagen, Hilden, Germany) using 5-mm stainless beads at 100 Hz for 1.5 minutes. The sample was then centrifuged for 2 minutes at 12,000 RCF to remove any debris or particulate matter. The supernatant was collected and diluted 1:4 in 0.1% Trixton X-100 in PBS before measurement. Triglyceride GPO-PAP Kit (Mti-diagnostics GmbH, Idstein, Germany) was used to measure the triglyceride concentration according to the manufacturer's instructions. The absorbance was measured at a wavelength of 540nm with an Ensight multimode plate reader (Perkin-Elmer, Massachusetts, USA).

3.8 Micro-ultrasound Image Analysis

The ultrasound B-mode scan images of the liver (3 images per sample acquired from longitudinal projection) were used for the evaluation of the Hepatic – Renal ratio on ImageJ. A region of interest (ROI) was drawn on the liver parenchyma as well as on corresponding portion of the renal cortex (Figure 5). These two ROI were drawn at the same depth for both organs and as close to the centre of the image as possible in order to ensure similar echo intensity attenuation for both regions and avoid borderline echo distortion. The mean grey intensity of the hepatic ROIs was averaged across 3 images per mouse to obtain a hepatic ROI value for each mouse, similarly the value for the renal ROI of each mouse was calculated in the same manner. The hepatic ROI value was divided by the renal ROI value obtained for each mouse to derive the Hepatic – Renal ratio (H/R). H/R ratio is considered an indirect parameter for quantifying liver fat content. The underlying premise of this assessment being that fat in the liver increases the echogenicity of the liver, making the liver parenchyma to be brighter than the adjacent kidney, which translates to a higher value for H/R ratio, when measured.

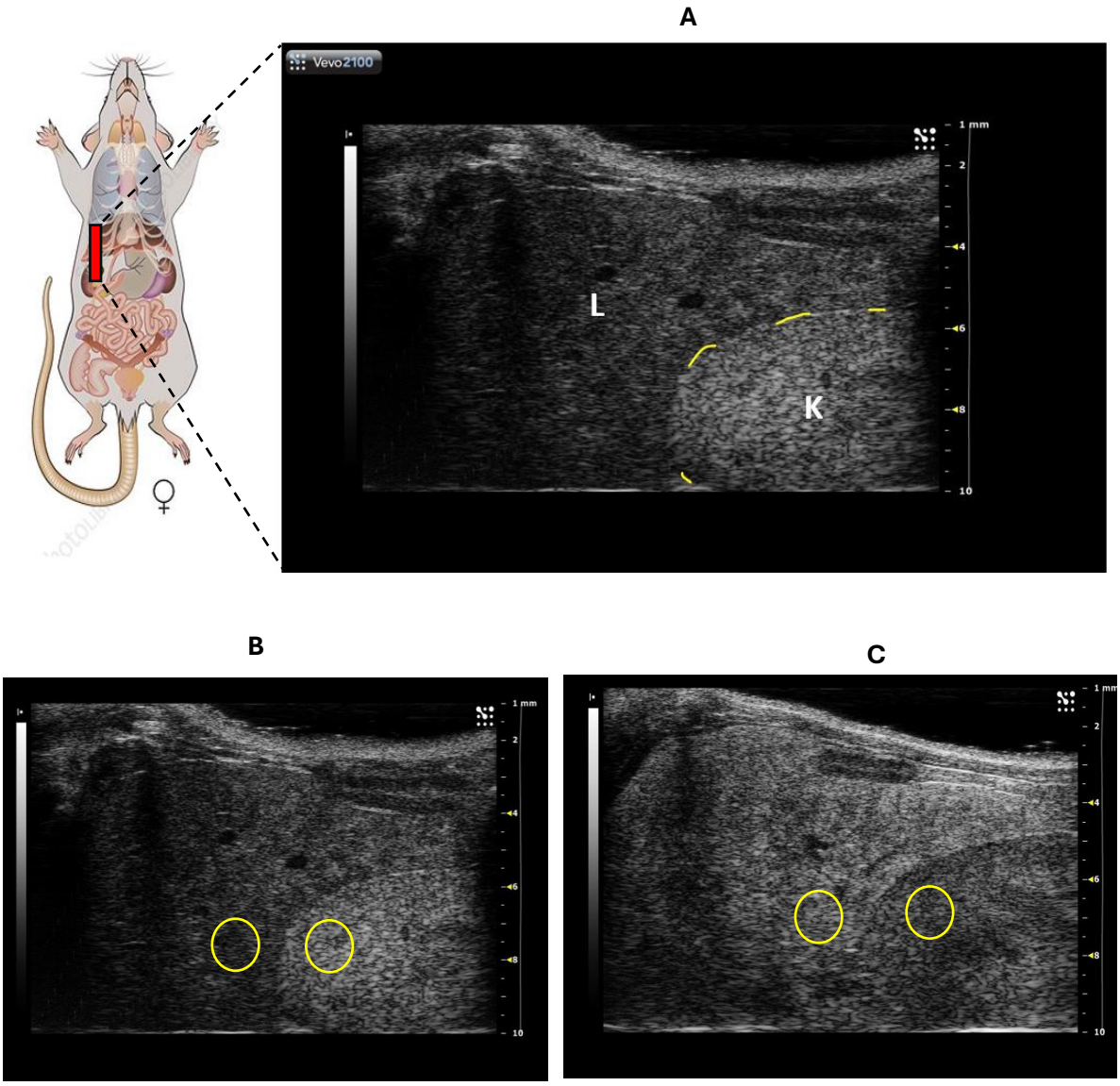

Figure 5: (A) Longitudinal projection B-mode image of mouse liver showing the medial lobe of the liver (L) and the right kidney (K) both separated by the broken yellow line. The red horizontal line on the mouse shows the orientation of the probe on the mouse for image acquisition. **(B)** and **(C)** are representative images of normal and fatty liver respectively, with the two yellow circles in each image depicting the size and level of the renal and hepatic ROI, used in calculating the H/R ratio.

3.9 Statistical Analysis

Statistical analysis was carried out using GraphPad Prism 10.2 software (GraphPad Software, Boston, USA). The Shapiro-Wilk test was used to test for normal distribution of

the data, and statistical test was chosen depending on the result of the test for normality. Unpaired *t*-test or Mann-Whitney test was used to determine the statistical significance between two groups at single time point, and two-way ANOVA for multiple time points. Pearson correlation coefficient (r) was used for the correlation analysis. The threshold for statistical significance was set at $p<0.05$. Results were expressed as mean ± SD.

4. RESULTS

4.1. High fat diet induces increase in body fat

To establish a model of diet-induced steatosis, we monitored the body weight, body composition and visceral fat accumulation in the mice fed with high fat diet as well as those on normal chow. Overall, the mice fed with high fat diet showed a modest, but significant increase in body weight compared to the chow mice (FC=1.10, p=0.13) (Figure 6A). There was no significant difference between the two groups at the baseline and the modest increase observed in the first two weeks (FC= 1.09, p=0.022) was lost in the third week. The increase in body weight between the groups was again significant in the fourth and fifth week (FC=1.09, p=0.031) and was increasingly more significant in weeks six through week 12 (FC=1.10 – 1.14, p=0.009 – 0.004). Furthermore, the mice on high fat diet had significantly greater percentage of body fat than those on chow diet (FC=1.50, p=<0.001) (Figure 6B). Although there was no significant difference in the body fat between the groups at the baseline measurement, with time, however, the mice on high fat diet accumulated more body fat than the mice on chow diet, and this was a consistent observation throughout the duration of the study. Similarly, the gonadal fat pads isolated from the mice on high fat diet after euthanasia, weighed significantly more than those from the chow diet (FC=1.83, p=<0.001) (Figure 6C). These findings indicate that over time, high fat diet consumption leads to an increase in body weight, fat mass and visceral fat accumulation.

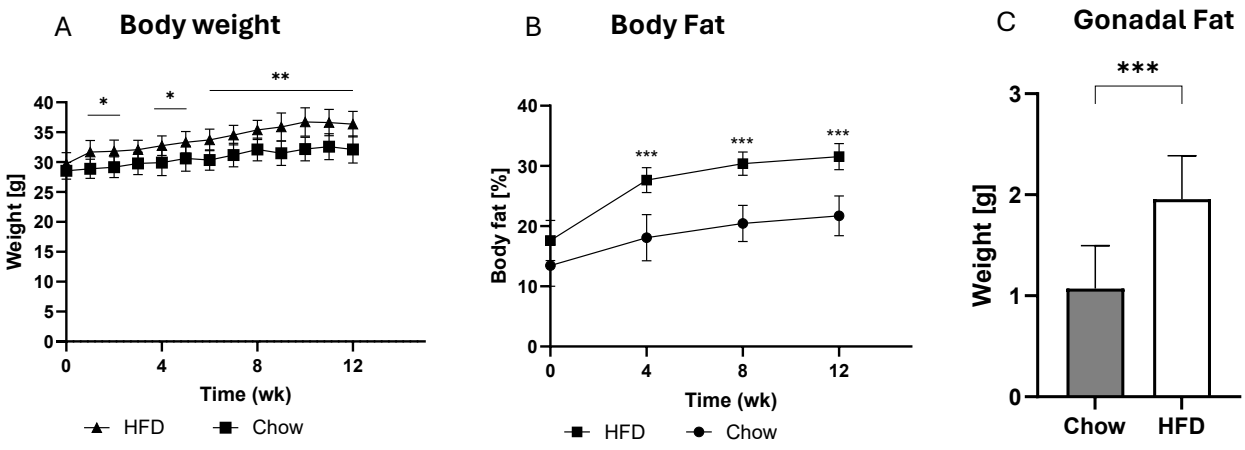

Figure 6: Mice on high fat diet (HFD) showed significant increase in ***(A*)** body weight ***(B)*** Body fat position and ***(C)*** Gonadal fat, when compared to those on chow diet. * P=0.022 – 0.031, ** P=0.004 – 0.009, *** P<0.001

4.2. Prolonged consumption of high fat diet induces the accumulation of fat in the liver but not in the kidney.

We measured the weights of the liver and kidney of the mice on high fat diet and chow diet at sacrifice, to determine possible alterations in organ size due to the diet. The liver of the mice on high fat diet weighed significantly more than that of the mice on chow diet (FC= 1.64, p=0.023) (Figure 7E). As expected, there was no significant difference between the weights of the kidney of both group (Figure 7F). Further investigation on the H&E-stained liver tissues of the groups revealed increased amounts of visible lipid droplets (Microvesicular and macrovesicular steatosis) in the liver of the mice on high fat diet compared to the chow diet group (figure 7A-B). The level of macro- and microvesicular steatosis in the liver parenchyma was quantified by a recently developed and validated deep learning-based image analysis model trained to accurately detect and quantify tissue areas containing lipid droplets in H&E-stained sections of mouse liver (Mairinoja et al., 2023). The result of the evaluation showed that on average, macrovesicular steatosis accounted for 57% of the liver tissue in the high fat diet mice as against less than 2% in the chow diet group (p=<0.001) (figure 7G). Similarly, microvesicular steatosis accounted for 38% of the

liver tissue in the high fat diet group compared to about 3% of the chow group's (p=<0.001) (Figure 7H). Meanwhile, histological analysis of the H&E-stained kidney tissues revealed normal structure and no significant difference between the mice on high fat diet and those on chow (Figure 7C-D). Together, these results suggest that while high fat diet consumption for the duration of this experiment resulted in hepatic steatosis and significant increase in liver weight, it did not induce any observable change in the histology and size of the kidney. In line with the foregoing, the liver triglyceride concentration in the mice on high fat diet was observed to be significantly higher than those on chow diet (FC=3.48, p=<0.001) (Figure 7I)

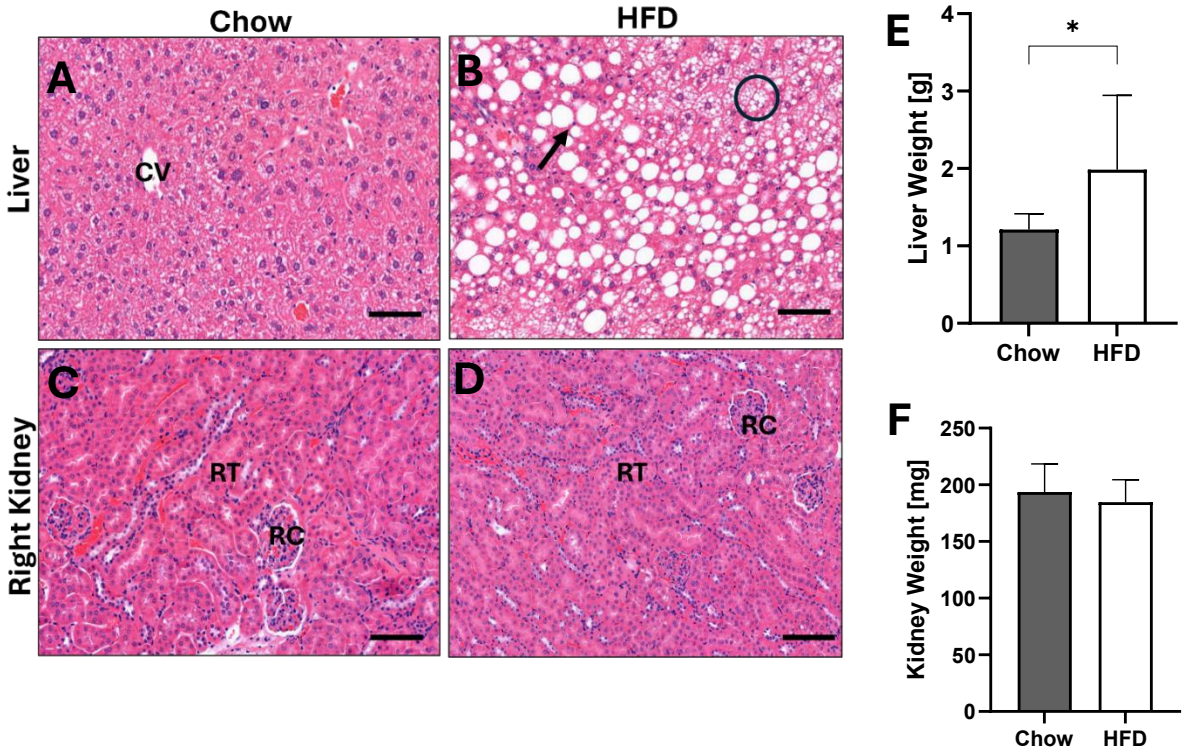

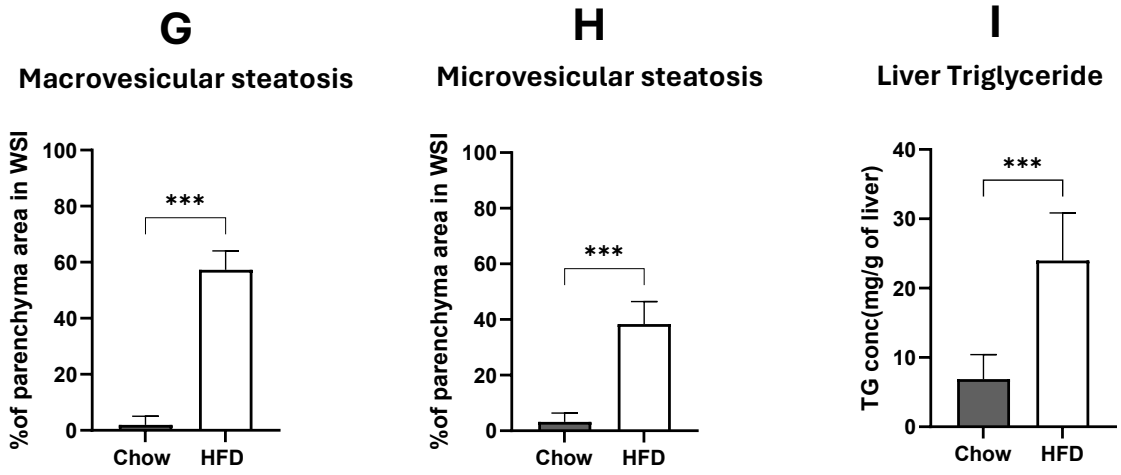

Figure 7: High fat diet induces structural changes in the liver but not the kidneys (A-D): Representative images of haematoxylin & eosin-stained liver tissue and the right kidney showing **(A)** homogeneous parenchyma with normal hepatocytes in chow mice **(B):** macrovesicular lipid droplets **(arrow)** and microvesicular lipid droplets **(circle)** in HFD mice. (C-D): Normal kidney histology with renal corpuscle (RC) and renal tubules (RT) for (C) chow and (D) HFD. (E) weight of the liver **(F):** weight of the right kidney. (G-H): Image analysis by the deep learning model showing significant increase in **(G)** Macrovesicular steatosis in the liver of the mice on high fat diet (HFD) and **(H)** Microvesicular steatosis in the liver of the mice on HFD. **(I)** significant increase in the liver triglyceride content of the mice in HFD. Scale bar: 100µm (A-D). * P=0.23, *** P<0.001. CV, central vein; HFD, High fat diet.

4.3. Quantitative micro-ultrasound can discriminate between healthy and fatty liver

To determine if quantitative micro-ultrasound technique can distinguish fatty liver from normal liver, we analysed the B-mode ultrasound images of the liver of the mice on high fat diet and normal chow (figure 8A), by using ImageJ software to measure the mean grey intensities of the liver and right kidney, from which we derived their Hepatic – Renal ratio (H/R). The result of the analysis revealed a significant increase in the H/R values of the mice on high fat diet compared to the chow group (FC=2.36, p=<0.001) and this was a consistent finding over the 12 weeks duration of the experiment (Figure 8B). At the

baseline, there was no significant difference between the high fat diet and chow group, however, by the fourth week, the significant difference between the groups was already evident (FC=2.25, p=0.004) and by the 8th week the difference between the groups was even more significant (FC=2.65, p=<0.001), and the same can be said for the difference observed in week 12 (FC=2.85, p=0.004). These data suggest that this technique can consistently differentiate fatty liver from a healthy liver.

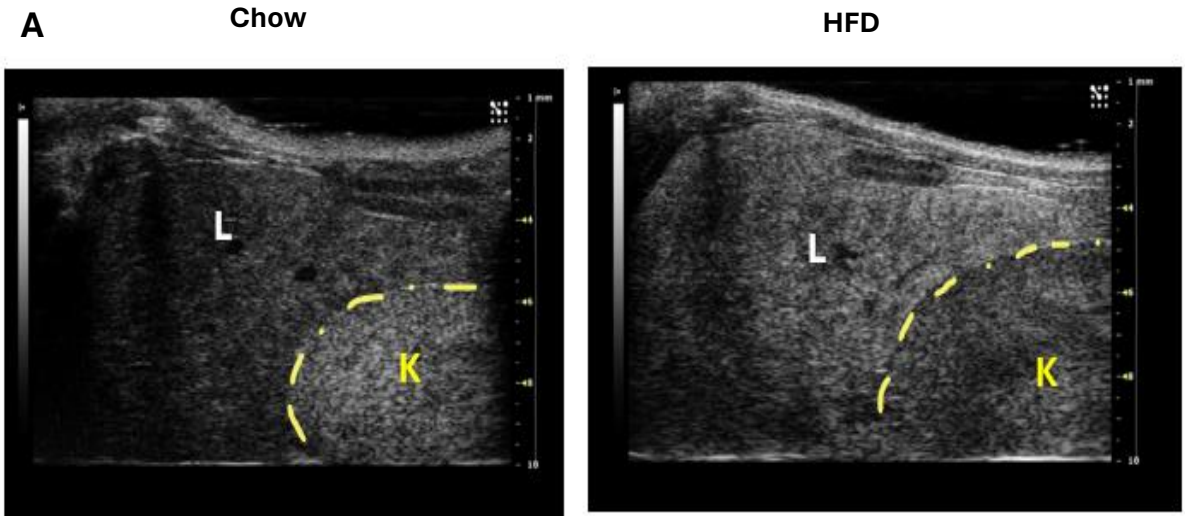

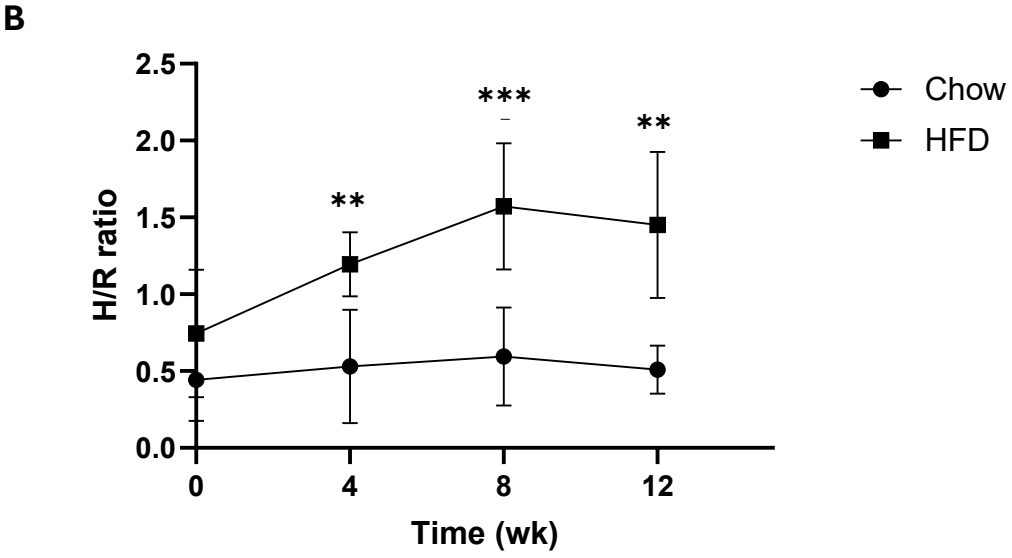

Figure 8: (A) Representative Ultrasound images of mice liver on chow and high fat diet (HFD) showing the observable difference between a healthy and fatty liver as indicated by their different grey intensities. The border between the liver (L) and kidney (K) is outlined in yellow broken line **(B)** The hepatic-renal ratio (H/R) of mice on HFD significantly increased compared to the chow diet, at different time points. ** P=0.004, *** P<0.001

4.4. Serum ALT activity reflects fat accumulation in the liver

To corroborate the histologic findings of hepatic steatosis and the attendant increase in triglyceride content of hepatic tissues of the mice on high fat diet, we measured the serum ALT activity of both groups, and as expected, the serum ALT level was significantly higher in the high fat diet group compared to the chow group (FC=6.35, p=<0.001) (Figure 9). This result is indicative of liver damage as a result of the abnormal accumulation of fat in the liver.

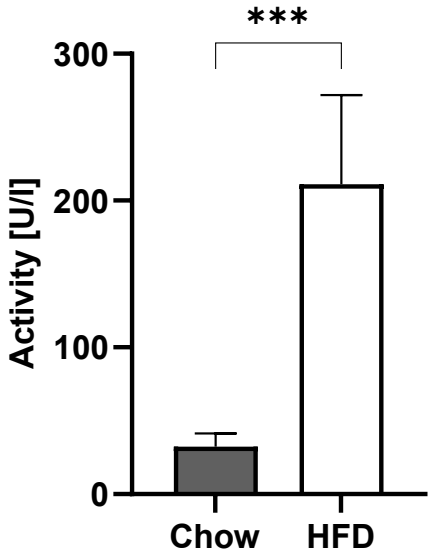

Figure 9: Serum ALT; Compared to the mice on chow diet, the serum ALT activity in the high fat diet mice was significantly higher. *** P<0.001

4.5. Hepatic-Renal ratio correlates with other biomarkers of hepatic steatosis

The hepatic-Renal ratio derived from quantitative analysis of ultrasound images was correlated with other established biomarkers of hepatic steatosis including the body fat composition, liver triglyceride concentration, serum ALT activity and histological image analysis of the liver, in order to validate the accuracy and reliability of this technique. The results of the analyses showed a positive correlation between the body fat and H/R ratio (r=0.62, p=0.058) (figure 10A), a weak correlation between H/R ratio and liver triglyceride content (r=0.46, p=0.1827) (figure 10B), a strong positive correlation between H/R ratio and serum ALT (r=0.92, p=<0.001) (figure 10C), and a strong positive correlation between H/R ratio and the histological image analysis (r=0.88, p=<0.001) (figure 10D). A correlation matrix summarizing all the analyses performed is presented in figure 10E

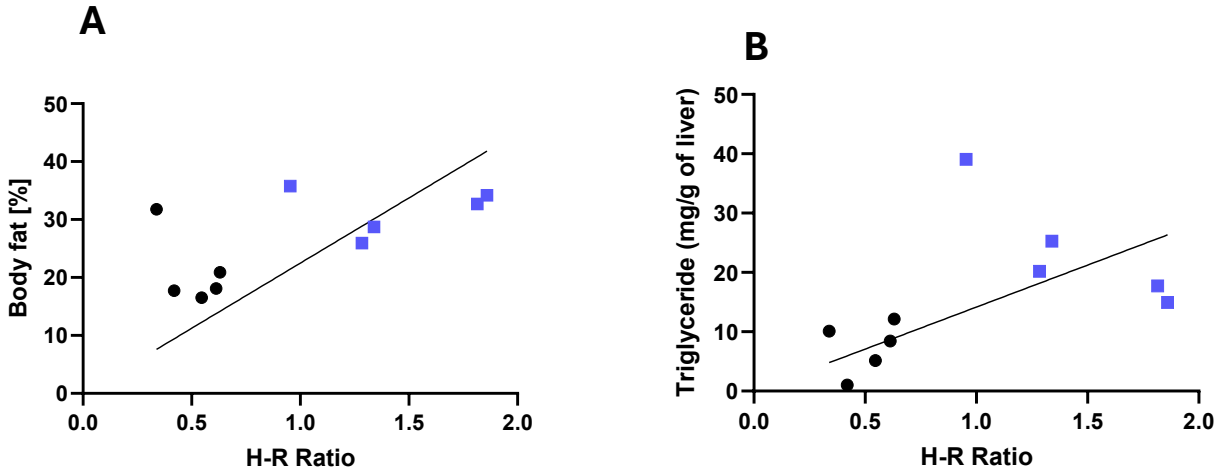

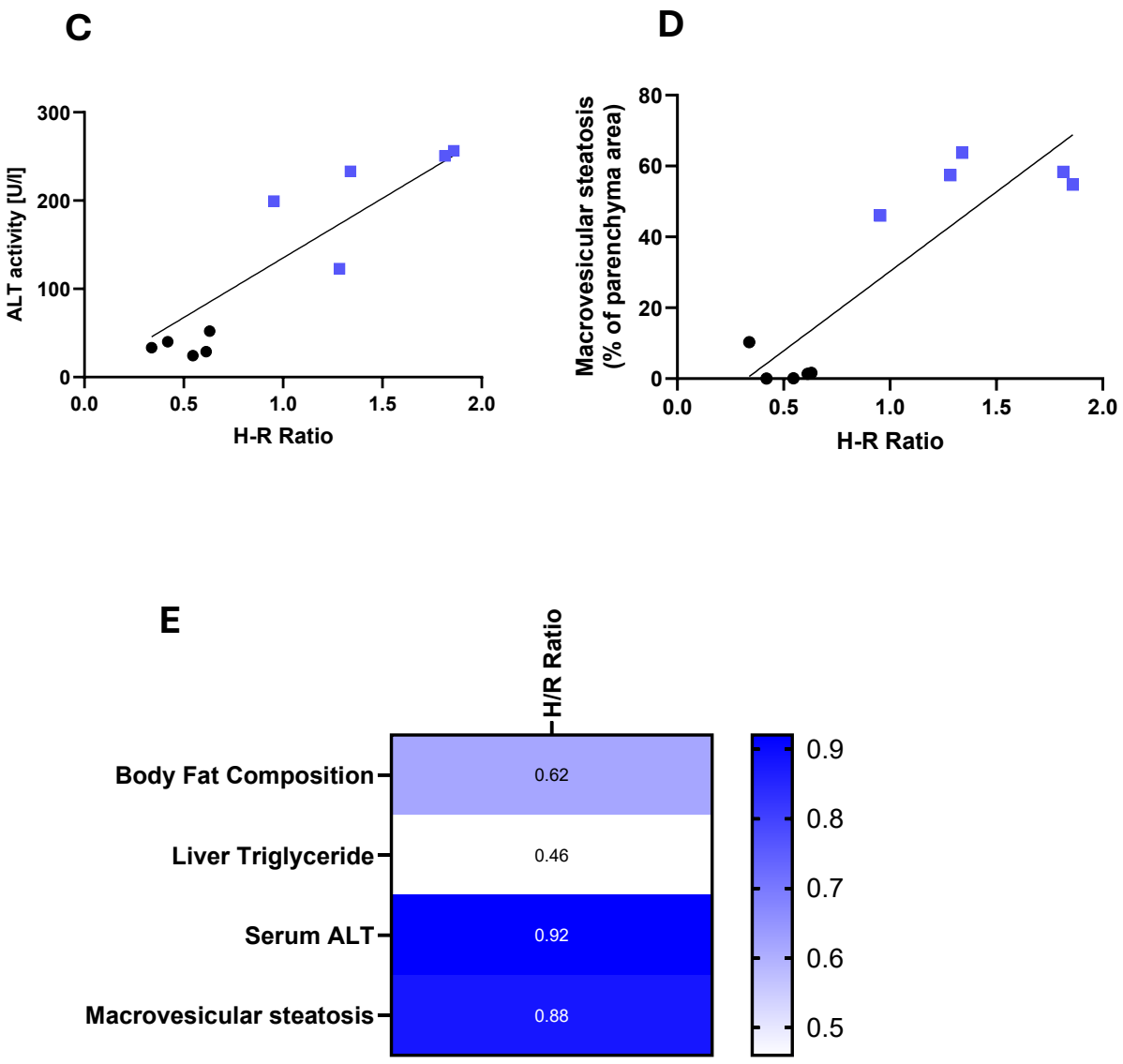

Figure 10: (A-D) Pearson correlation curve between hepatic-renal ratio (H/R) and **(A)** Body fat composition (r=0.62, p=0.058) **(B)** Liver triglyceride concentration (r=0.46, p=0.1827) **(C)** Serum ALT (r=0.92, p=<0.001) **(D)** Histological analysis by the deep learning model (r=0.88, p=<0.001). **(E):** Correlation matrix of the analyses. **Black circles** represent mice on chow and **blue squares** represent mice on HFD **(A-D)**

5. DISCUSSION

This study was aimed at evaluating whether quantitative micro-ultrasound technique could be used to follow the development of fatty liver disease in mouse over time, and whether this technique is sensitive enough to accurately differentiate fatty liver from the control *in vivo*.

Diet-induced mouse model of NAFLD as employed by this study, is a well characterized model of the disease known to recapitulate key features of its pathophysiology (Flessa et al., 2022), and as expected, histologic evaluation confirmed the development of hepatic steatosis in the mice. This observation was further substantiated by the increase in body fat, liver triglyceride concentration and serum ALT level. Furthermore, quantitative analysis of their ultrasound images revealed a clear difference between both groups.

Throughout the 12-week feeding period, the body weights of the chow and HFD mice increased. However, the difference in the body weight of the HFD mice compared to the chow, were mostly mild and sometimes non-existent. This was similar to the report by Eccleston et al, who observed that male C57BL/6 mice on HFD for 16 weeks developed hepatic steatosis, but showed no significant body weight difference compared to control (Eccleston et al., 2011). Interestingly, when this strain of mice were fed on high fat diet for longer period, the difference in their body weight compared to the control mice became significant only after the first 3 months, and even then, about 25% of the HFD mice had bodyweight similar to the control mice after 9months (Burcelin et al., 2002). Thus, it is likely that the observed effect of HFD on the body weight of C57BL/6 inbred mouse strain, may be dependent on the duration of administration and strain-specific epigenetic modifications affecting the gene expression pattern of Scd-1 in the liver (Fourmestraux et al., 2004; Flessa et al., 2022). Furthermore, the specific nutritional composition of the high fat diet has been reported to exert variable effect on the metabolic profile of the rodent. This variability appears to be dependent on the source and quantity of sucrose, fat, and protein in the diet (Janoschek et al., 2023). It is therefore possible that the composition of the high fat diet used in this study, played a role in the body weight of the mice.

In clinical practice, conventional ultrasonography is used in the evaluation of hepatic steatosis, and diagnosis primarily relies on the visual assessment of the relative echogenicity (brightness) of the liver parenchyma compared to the renal cortex, as well as the degree of ultrasonic attenuation (Strauss et al., 2007; Hernaez et al., 2011b). The principle underlying this qualitative assessment being that accumulation of fat in the liver alters the acoustic impedance of the parenchyma, and this manifests as a number of characteristic alterations in the ultrasound image. However, this method is highly subjective as interpretation tends to vary depending on the skill of the observer (Strauss et al., 2007). To address this limitation, quantitative analysis of the liver echogenicity in ultrasound images, the so-called hepatic-renal ratio (H/R), has been proposed as a valid alternative (Mancini et al., 2009; Martín-Rodríguez et al., 2014). Validation of this technique in preclinical model is necessary to facilitate longitudinal studies that will help unravel the pathophysiology of the disease. A major drawback of the H/R technique is that results may be compromised in cases where the kidney (the reference organ for comparison) is diseased or absent. In this study, however, the result of the histological evaluation showed that the kidneys of the mice on high fat diet were normal and identical in structure and weight to that of the chow. Interestingly, visual evaluation of their ultrasound images revealed a significant difference in the kidney echogenicity of the HFD mice compared to the chow, as the HFD kidneys were darker in appearance at all measured time points except during the first time point where their appearances were identical. Since the experimental conditions were the same for both groups, and their kidneys have been shown to be healthy and structurally similar, it is likely that the observed phenomenon may be due to how the microprocessor within the ultrasound device assigns gray-scale values to the echoes returning from tissues to the transducer (Zander et al., 2020). It is my hypothesis that because the bit depth of the ultrasound system is limited in display to 256 shades of gray (Long et al., 2020), the software adjusts the echo intensity of returning waves to fit within the 256 gradation in such a way that the true difference in the echogenicity between adjacent tissues are accurately reflected in the displayed image. This assumption is based on the fact that the image acquisition for both groups was done with the default system settings of the same device and on the same days, yet the observation was consistent at different time points.

The hepatic-renal ratio, derived from the translation of the echogenicity of liver and kidney into numerical data using ImageJ software, was used to evaluate the sensitivity of this quantitative technique in distinguishing fatty and normal liver in mice. We learnt from the results that this technique is sensitive enough to detect the early onset of fatty liver disease as there was statistically significant difference between the chow and HFD groups as early as the 4^{th} week of the experiment and for the duration of the study. This was consistent with the results of a previous study quantifying liver fat content with ultrasound (Zhang et al., 2014). Despite their varying degrees of sensitivity and specificity for the disease, liver triglyceride concentration and serum ALT activity are among the currently available biomarkers of NAFLD (Tomizawa et al., 2014; Wong et al., 2018). Similar to the report of a recent study (Adam et al., 2018b), the liver triglyceride concentration of the HFD mice was observed to be nearly 3.5 times higher than in the chow mice, which was indicative of hepatic steatosis. Additionally, the serum ALT level which was 6.3 times higher in the HFD mice, signified liver damage potentially caused by the excessive accumulation of fat in the liver (Martin-Rodriguez et al., 2017). Thus, it is evident that these biomarkers are in agreement with the results of the H/R technique.

Histological analysis is the reference standard for NAFLD assessment, but a deep learning-based image analysis model in conjunction with other biomarkers of NAFLD was used to validate the quantitative micro-ultrasound technique in this study. However, the performance of the deep learning-based model has been validated and shown to reliably replicate the independent evaluation of expert pathologists, and therefore it represents an objective, efficient and cost-effective alternative (Mairinoja et al., 2023). Pearson correlation analysis of H/R ratio and body fat composition, liver triglyceride, serum ALT and the image analysis model revealed a positive correlation with these parameters, although with varying degree of statistical significance and strength, which may be due to the variations in the samples and limited sample size. Nonetheless, H/R ratio significantly correlated with the deep-learning image analysis model ($r=0.88$, $p=<0.001$), and because the other validation parameters also correlated positively with H/R ratio on a general level, we can safely consider these as sufficient basis to conclude that the H/R technique is a feasible quantitative and non-invasive approach that is sensitive enough to detect the accumulation of fat in the liver.

In this study, high fat diet was used to induce hepatic steatosis in male mice, and quantitative micro-ultrasound technique demonstrably distinguished fatty liver from their healthy controls on a consistent basis. The next step will be to verify if this finding holds true in other diet-induced models as well as in chemically induced models and in genetically modified models, where the inherent heterogeneity of NAFLD in these phenotypes will provide valuable insights on the generalizability of the H/R technique. Furthermore, the technical complexity and time-consuming nature of micro-ultrasound imaging necessitated the use of a relatively small sample size, which was however, adequate for this study design. Future studies could explore possible means of optimizing the imaging protocol in order to facilitate the study of larger sample cohorts with this technique. Again, beyond detecting the presence of hepatic steatosis, determining the severity of the disease by stratifying intrahepatic fat into the different grades of hepatic steatosis is also important for comprehensive evaluation of therapeutic interventions in NAFLD. This is a noted limitation in this study and could be the basis for future studies.

Nevertheless, there are currently no other reliable noninvasive and safe methods for longitudinal study of the preclinical models of NAFLD in vivo. Previous studies have traditionally relied on euthanizing the animals at different time point intervals during the course of the study in order to characterize the observable features (Fernández-Domínguez et al., 2011; Rowles et al., 2019), an approach which raises ethical concerns and limits the ability to track individual animal responses overtime and assess variability within groups. Based on the results of this study, it is evident that quantitative micro-ultrasound technique makes it possible to follow the development of hepatic steatosis in individual animals over time. This not only significantly contributes towards the effort to replace the more invasive methods, but also reduces the number of animals required in research in line with the 3R framework.

6. CONCLUSION

Quantitative micro-ultrasound is a feasible technique for monitoring the development of hepatic steatosis *in vivo*, as our data indicate that it is sensitive enough to detect differences between normal and fatty liver as early as the four weeks after commencing the high fat diet intervention. Further studies are necessary to show how repeatable the technique is in other preclinical models of NAFLD.

7. ACKNOWLEDGEMENT

I was blessed with the good fortune of being supervised for my thesis by the best team there is, and I would like to express my sincere gratitude to my amiable supervisors; Adjunct Professor Leena Strauss, Post Doctoral Researcher Hanna Heikelä and Doctoral Researcher Laura Mairinoja, without whose guidance and patience this project would not have been a success. I am grateful that you always and unfailingly made time for me every time I came running to you with my plethora of questions, and this was despite your very busy schedule. I was able to actualize this work only because I stood on your shoulders. I am grateful for your mentorship, and it has been such a pleasure working with you.

I would also like to thank the group leader of Endocrine Signalling Consortium, Professor Matti Poutanen for the opportunity to be a part of this exciting project, and for your insightful questions and feedback during the meetings.

Many thanks to all the researchers in Mediciina C5, notably; Opeyemi Olotu, Guillermo Martinez, Ammar Ahmenadi, Krisztina Kukoricza, Raktim Hati, Inka Raimoranta and Samuli Laasanen. Thank you for being such wonderful friends and supportive colleagues.

To all my teachers and course mates in the BIMA program, thank you for sharing this journey with me, and what a journey it has been these two years!

I am forever indebted to the unconditional love and nurturing care of my parent and siblings; Elder Ekwe Igwe, Mother Elizabeth Ekwe, Chukwuemeka, Ifeanyi, Oluchi, Kelech and Onyekachi – including their spouses and kids. Your unparalleled selflessness towards me and your exemplary lifestyle, paved the way for me to get to this point. I am eternally grateful for the gift of you, and if ever I have to choose my parent and siblings, I will choose you again and again and again!

Above all, to Jesus Christ my Saviour, the giver of life and all good things, thank you Lord for the gift of youth and a sound mind.

8. REFERENCES

Abu-Shanab, A., & Quigley, E. M. M. (2010). The role of the gut microbiota in nonalcoholic fatty liver disease. *Nature Reviews. Gastroenterology & Hepatology*, *7*(12), 691–701. https://doi.org/10.1038/nrgastro.2010.172

Adam, M., Heikelä, H., Sobolewski, C., Portius, D., Mäki-Jouppila, J., Mehmood, A., Adhikari, P., Esposito, I., Elo, L. L., Zhang, F.-P., Ruohonen, S. T., Strauss, L., Foti, M., & Poutanen, M. (2018a). Hydroxysteroid (17β) dehydrogenase 13 deficiency triggers hepatic steatosis and inflammation in mice. *The FASEB Journal*, *32*(6), 3434–3447. https://doi.org/10.1096/fj.201700914R

Adam, M., Heikelä, H., Sobolewski, C., Portius, D., Mäki-Jouppila, J., Mehmood, A., Adhikari, P., Esposito, I., Elo, L. L., Zhang, F.-P., Ruohonen, S. T., Strauss, L., Foti, M., & Poutanen, M. (2018b). Hydroxysteroid (17β) dehydrogenase 13 deficiency triggers hepatic steatosis and inflammation in mice. *FASEB Journal: Official Publication of the Federation of American Societies for Experimental Biology*, *32*(6), 3434–3447. https://doi.org/10.1096/fj.201700914R

Argo, C. K., & Caldwell, S. H. (2009). Epidemiology and Natural History of Non-Alcoholic Steatohepatitis. *Clinics in Liver Disease*, *13*(4), 511–531. https://doi.org/10.1016/j.cld.2009.07.005

Barisoni, L., Lafata, K. J., Hewitt, S. M., Madabhushi, A., & Balis, U. G. J. (2020). Digital pathology and computational image analysis in nephropathology. *Nature Reviews Nephrology*, *16*(11), Article 11. https://doi.org/10.1038/s41581-020-0321-6

Bell-Anderson, K. S., Aouad, L., Williams, H., Sanz, F. R., Phuyal, J., Larter, C. Z., Farrell, G. C., & Caterson, I. D. (2011). Coordinated improvement in glucose tolerance, liver steatosis and obesity-associated inflammation by cannabinoid 1 receptor antagonism in fat Aussie mice. *International Journal of Obesity*, *35*(12), Article 12. https://doi.org/10.1038/ijo.2011.55

Bence, K. K., & Birnbaum, M. J. (2020). Metabolic drivers of non-alcoholic fatty liver disease. *Molecular Metabolism*, *50*, 101143. https://doi.org/10.1016/j.molmet.2020.101143

Burcelin, R., Crivelli, V., Dacosta, A., Roy-Tirelli, A., & Thorens, B. (2002). Heterogeneous metabolic adaptation of C57BL/6J mice to high-fat diet. *American Journal of Physiology-Endocrinology and Metabolism*. https://doi.org/10.1152/ajpendo.00332.2001

Chalasani, N., Younossi, Z., Lavine, J. E., Charlton, M., Cusi, K., Rinella, M., Harrison, S. A., Brunt, E. M., & Sanyal, A. J. (2018). The diagnosis and management of nonalcoholic fatty liver disease: Practice guidance from the American Association for the Study of Liver Diseases. *Hepatology*, *67*(1), 328. https://doi.org/10.1002/hep.29367

Chen, X., Wang, X., Zhang, K., Fung, K.-M., Thai, T. C., Moore, K., Mannel, R. S., Liu, H., Zheng, B., & Qiu, Y. (2022). Recent advances and clinical applications of deep learning

in medical image analysis. *Medical Image Analysis*, *79*, 102444. https://doi.org/10.1016/j.media.2022.102444

Cohen, J. C., Horton, J. D., & Hobbs, H. H. (2011). Human Fatty Liver Disease: Old Questions and New Insights. *Science (New York, N.Y.)*, *332*(6037), 1519. https://doi.org/10.1126/science.1204265

Di Lascio, N., Avigo, C., Salvati, A., Martini, N., Ragucci, M., Monti, S., Prinster, A., Chiappino, D., Mancini, M., D'Elia, D., Ghiadoni, L., Bonino, F., Brunetto, M. R., & Faita, F. (2018). Steato-Score: Non-Invasive Quantitative Assessment of Liver Fat by Ultrasound Imaging. *Ultrasound in Medicine & Biology*, *44*(8), 1585–1596. https://doi.org/10.1016/j.ultrasmedbio.2018.03.011

Di Lascio, N., Kusmic, C., Stea, F., Lenzarini, F., Barsanti, C., Leloup, A., & Faita, F. (2018). Longitudinal micro-ultrasound assessment of the ob/ob mouse model: Evaluation of cardiovascular, renal and hepatic parameters. *International Journal of Obesity*, *42*(3), Article 3. https://doi.org/10.1038/ijo.2017.219

Eccleston, H. B., Andringa, K. K., Betancourt, A. M., King, A. L., Mantena, S. K., Swain, T. M., Tinsley, H. N., Nolte, R. N., Nagy, T. R., Abrams, G. A., & Bailey, S. M. (2011). Chronic Exposure to a High-Fat Diet Induces Hepatic Steatosis, Impairs Nitric Oxide Bioavailability, and Modifies the Mitochondrial Proteome in Mice. *Antioxidants & Redox Signaling*, *15*(2), 447–459. https://doi.org/10.1089/ars.2010.3395

Eslam, M., Valenti, L., & Romeo, S. (2018). Genetics and epigenetics of NAFLD and NASH: Clinical impact. *Journal of Hepatology*, *68*(2), 268–279. https://doi.org/10.1016/j.jhep.2017.09.003

Fernández-Domínguez, I., Echevarria-Uraga, J. J., Gómez, N., Luka, Z., Wagner, C., Lu, S. C., Mato, J. M., Martínez-Chantar, M. L., & Rodríguez-Cuesta, J. (2011). High-Frequency Ultrasound Imaging for Longitudinal Evaluation of Non-Alcoholic Fatty Liver Disease Progression in Mice. *Ultrasound in Medicine & Biology*, *37*(7), 1161–1169. https://doi.org/10.1016/j.ultrasmedbio.2011.04.012

Flessa, C.-M., Nasiri-Ansari, N., Kyrou, I., Leca, B. M., Lianou, M., Chatzigeorgiou, A., Kaltsas, G., Kassi, E., & Randeva, H. S. (2022). Genetic and Diet-Induced Animal Models for Non-Alcoholic Fatty Liver Disease (NAFLD) Research. *International Journal of Molecular Sciences*, *23*(24), Article 24. https://doi.org/10.3390/ijms232415791

Fourmestraux, V. de, Neubauer, H., Poussin, C., Farmer, P., Falquet, L., Burcelin, R., Delorenzi, M., & Thorens, B. (2004). Transcript Profiling Suggests That Differential Metabolic Adaptation of Mice to a High Fat Diet Is Associated with Changes in Liver to Muscle Lipid Fluxes *. *Journal of Biological Chemistry*, *279*(49), 50743–50753. https://doi.org/10.1074/jbc.M408014200

Friedman, S. L., Neuschwander-Tetri, B. A., Rinella, M., & Sanyal, A. J. (2018). Mechanisms of NAFLD development and therapeutic strategies. *Nature Medicine*, *24*(7), 908–922. https://doi.org/10.1038/s41591-018-0104-9

Haas, J. T., Francque, S., & Staels, B. (2016). Pathophysiology and Mechanisms of Nonalcoholic Fatty Liver Disease. *Annual Review of Physiology*, *78*(Volume 78, 2016), 181–205. https://doi.org/10.1146/annurev-physiol-021115-105331

Hannah Jr., W. N., & Harrison, S. A. (2016). Noninvasive imaging methods to determine severity of nonalcoholic fatty liver disease and nonalcoholic steatohepatitis. *Hepatology*, *64*(6), 2234–2243. https://doi.org/10.1002/hep.28699

Hernaez, R., Lazo, M., Bonekamp, S., Kamel, I., Brancati, F. L., Guallar, E., & Clark, J. M. (2011a). Diagnostic Accuracy and Reliability of Ultrasonography for the Detection of Fatty Liver: A Meta-Analysis. *Hepatology (Baltimore, Md.)*, *54*(3), 1082–1090. https://doi.org/10.1002/hep.24452

Hernaez, R., Lazo, M., Bonekamp, S., Kamel, I., Brancati, F. L., Guallar, E., & Clark, J. M. (2011b). Diagnostic Accuracy and Reliability of Ultrasonography for the Detection of Fatty Liver: A Meta-Analysis. *Hepatology (Baltimore, Md.)*, *54*(3), 1082–1090. https://doi.org/10.1002/hep.24452

Ho, J., Ahlers, S. M., Stratman, C., Aridor, O., Pantanowitz, L., Fine, J. L., Kuzmishin, J. A., Montalto, M. C., & Parwani, A. V. (2014). Can Digital Pathology Result In Cost Savings? A Financial Projection For Digital Pathology Implementation At A Large Integrated Health Care Organization. *Journal of Pathology Informatics*, *5*, 33. https://doi.org/10.4103/2153-3539.139714

Ibrahim, S. H., Hirsova, P., Malhi, H., & Gores, G. J. (2016). Animal Models of Nonalcoholic Steatohepatitis: Eat, Delete, and Inflame. *Digestive Diseases and Sciences*, *61*(5), 1325–1336. https://doi.org/10.1007/s10620-015-3977-1

Jacobs, A., Warda, A.-S., Verbeek, J., Cassiman, D., & Spincemaille, P. (2016). An Overview of Mouse Models of Nonalcoholic Steatohepatitis: From Past to Present. *Current Protocols in Mouse Biology*, *6*(2), 185–200. https://doi.org/10.1002/cpmo.3

Jahn, S. W., Plass, M., & Moinfar, F. (2020). Digital Pathology: Advantages, Limitations and Emerging Perspectives. *Journal of Clinical Medicine*, *9*(11), 3697. https://doi.org/10.3390/jcm9113697

Janoschek, R., Handwerk, M., Hucklenbruch-Rother, E., Schmitz, L., Bae-Gartz, I., Kasper, P., Lackmann, J.-W., Kretschmer, T., Vohlen, C., Mesaros, A., Purrio, M., Quaas, A., Dötsch, J., & Appel, S. (2023). Heterogeneous effects of individual high-fat diet compositions on phenotype, metabolic outcome, and hepatic proteome signature in BL/6 male mice. *Nutrition & Metabolism*, *20*(1), 8. https://doi.org/10.1186/s12986-023-00729-0

Kiran, N., Sapna, F. N. U., Kiran, F. N. U., Kumar, D., Raja, F. N. U., Shiwlani, S., Paladini, A., Sonam, F. N. U., Bendari, A., Perkash, R. S., Anjali, F. N. U., & Varrassi, G. (2023). Digital Pathology: Transforming Diagnosis in the Digital Age. *Cureus*, *15*(9). https://doi.org/10.7759/cureus.44620

Lau, J. K. C., Zhang, X., & Yu, J. (2017). Animal models of non-alcoholic fatty liver disease: Current perspectives and recent advances. *The Journal of Pathology*, *241*(1), 36–44. https://doi.org/10.1002/path.4829

Long, Z., Zhou, W., Tradup, D. J., Stekel, S. F., Callstrom, M. R., & Hangiandreou, N. J. (2020). Systematic optimization of ultrasound grayscale imaging presets and its application in abdominal scanning. *Journal of Applied Clinical Medical Physics*, *21*(10), 192–199. https://doi.org/10.1002/acm2.13000

Mairinoja, L., Heikelä, H., Blom, S., Kumar, D., Knuuttila, A., Boyd, S., Sjöblom, N., Birkman, E.-M., Rinne, P., Ruusuvuori, P., Strauss, L., & Poutanen, M. (2023). Deep Learning-Based Image Analysis of Liver Steatosis in Mouse Models. *The American Journal of Pathology*, *193*(8), 1072–1080. https://doi.org/10.1016/j.ajpath.2023.04.014

Mancini, M., Prinster, A., Annuzzi, G., Liuzzi, R., Giacco, R., Medagli, C., Cremone, M., Clemente, G., Maurea, S., Riccardi, G., Rivellese, A. A., & Salvatore, M. (2009). Sonographic hepatic-renal ratio as indicator of hepatic steatosis: Comparison with 1H magnetic resonance spectroscopy. *Metabolism*, *58*(12), 1724–1730. https://doi.org/10.1016/j.metabol.2009.05.032

Martín-Rodríguez, J. L., Arrebola, J. P., Jiménez-Moleón, J. J., Olea, N., & González-Calvin, J. L. (2014). Sonographic quantification of a Hepato-Renal Index for the assessment of hepatic steatosis in comparison with 3T proton magnetic resonance spectroscopy. *European Journal of Gastroenterology & Hepatology*, *26*(1), 88. https://doi.org/10.1097/MEG.0b013e3283650650

Martin-Rodriguez, J. L., Gonzalez-Cantero, J., Gonzalez-Cantero, A., Arrebola, J. P., & Gonzalez-Calvin, J. L. (2017). Diagnostic accuracy of serum alanine aminotransferase as biomarker for nonalcoholic fatty liver disease and insulin resistance in healthy subjects, using 3T MR spectroscopy. *Medicine*, *96*(17), e6770. https://doi.org/10.1097/MD.0000000000006770

Robinson, K. E., & Shah, V. H. (2020). Pathogenesis and pathways: Nonalcoholic fatty liver disease & alcoholic liver disease. *Translational Gastroenterology and Hepatology*, *5*(0), Article 0. https://doi.org/10.21037/tgh.2019.12.05

Rowles, J. L., Han, A., Miller, R. J., Kelly, J. R., Applegate, C. C., Wallig, M. A., O'Brien, W. D., & Erdman, J. W. (2019). Low fat but not soy protein isolate was an effective intervention to reduce nonalcoholic fatty liver disease progression in C57BL/6J mice: Monitored by a novel quantitative ultrasound (QUS) method. *Nutrition Research*, *63*, 95–105. https://doi.org/10.1016/j.nutres.2018.12.003

Sahai, A., Malladi, P., Pan, X., Paul, R., Melin-Aldana, H., Green, R. M., & Whitington, P. F. (2004). Obese and diabetic db/db mice develop marked liver fibrosis in a model of nonalcoholic steatohepatitis: Role of short-form leptin receptors and osteopontin. *American Journal of Physiology. Gastrointestinal and Liver Physiology*, *287*(5), G1035-1043. https://doi.org/10.1152/ajpgi.00199.2004

Samji, N. S., Verma, R., & Satapathy, S. K. (2019). Magnitude of Nonalcoholic Fatty Liver Disease: Western Perspective. *Journal of Clinical and Experimental Hepatology*, *9*(4), 497–505. https://doi.org/10.1016/j.jceh.2019.05.001

Stephenson, K., Kennedy, L., Hargrove, L., Demieville, J., Thomson, J., Alpini, G., & Francis, H. (2018). Updates on Dietary Models of Nonalcoholic Fatty Liver Disease: Current Studies and Insights. *Gene Expression*, *18*(1), 5–17. https://doi.org/10.3727/105221617X15093707969658

Stockinger, P., Berlin, A., Kampik, D., Schmitt, C., Hillenkamp, J., Messinger, J. D., Herwig-Carl, M. C., & Ach, T. (2021). Correlation of in vivo/ex vivo imaging of the posterior eye segment. *Der Ophthalmologe : Zeitschrift Der Deutschen Ophthalmologischen Gesellschaft*, *118*(Suppl 2), 153–159. https://doi.org/10.1007/s00347-021-01439-9

Strauss, S., Gavish, E., Gottlieb, P., & Katsnelson, L. (2007). Interobserver and Intraobserver Variability in the Sonographic Assessment of Fatty Liver. *American Journal of Roentgenology*, *189*(6), W320–W323. https://doi.org/10.2214/AJR.07.2123

Takahashi, Y., Soejima, Y., & Fukusato, T. (2012). Animal models of nonalcoholic fatty liver disease/nonalcoholic steatohepatitis. *World Journal of Gastroenterology : WJG*, *18*(19), 2300–2308. https://doi.org/10.3748/wjg.v18.i19.2300

Teng, M. L., Ng, C. H., Huang, D. Q., Chan, K. E., Tan, D. J., Lim, W. H., Yang, J. D., Tan, E., & Muthiah, M. D. (2023). Global incidence and prevalence of nonalcoholic fatty liver disease. *Clinical and Molecular Hepatology*, *29*(Suppl), S32–S42. https://doi.org/10.3350/cmh.2022.0365

Tomizawa, M., Kawanabe, Y., Shinozaki, F., Sato, S., Motoyoshi, Y., Sugiyama, T., Yamamoto, S., & Sueishi, M. (2014). Triglyceride is strongly associated with nonalcoholic fatty liver disease among markers of hyperlipidemia and diabetes. *Biomedical Reports*, *2*(5), 633–636. https://doi.org/10.3892/br.2014.309

Van Herck, M. A., Vonghia, L., & Francque, S. M. (2017). Animal Models of Nonalcoholic Fatty Liver Disease-A Starter's Guide. *Nutrients*, *9*(10), 1072. https://doi.org/10.3390/nu9101072

Wong, V. W.-S., Adams, L. A., de Lédinghen, V., Wong, G. L.-H., & Sookoian, S. (2018). Noninvasive biomarkers in NAFLD and NASH — current progress and future promise. *Nature Reviews Gastroenterology & Hepatology*, *15*(8), 461–478. https://doi.org/10.1038/s41575-018-0014-9

Wu, J. Y., Tuomi, A., Beland, M. D., Konrad, J., Glidden, D., Grand, D., & Merck, D. (2016). Quantitative analysis of ultrasound images for computer-aided diagnosis. *Journal of Medical Imaging*, *3*(1), 014501. https://doi.org/10.1117/1.JMI.3.1.014501

Yang, M., Qi, X., Li, N., Kaifi, J. T., Chen, S., Wheeler, A. A., Kimchi, E. T., Ericsson, A. C., Rector, R. S., Staveley-O'Carroll, K. F., & Li, G. (2023). Western diet contributes to the pathogenesis of non-alcoholic steatohepatitis in male mice via remodeling gut

microbiota and increasing production of 2-oleoylglycerol. *Nature Communications*, *14*(1), Article 1. https://doi.org/10.1038/s41467-023-35861-1

Zander, D., Hüske, S., Hoffmann, B., Cui, X.-W., Dong, Y., Lim, A., Jenssen, C., Löwe, A., Koch, J. B. H., & Dietrich, C. F. (2020). Ultrasound Image Optimization ("Knobology"): B-Mode. *Ultrasound International Open*, *6*(1), E14–E24. https://doi.org/10.1055/a-1223-1134

Zhang, B., Ding, F., Chen, T., Xia, L.-H., Qian, J., & Lv, G.-Y. (2014). Ultrasound hepatic/renal ratio and hepatic attenuation rate for quantifying liver fat content. *World Journal of Gastroenterology : WJG*, *20*(47), 17985–17992. https://doi.org/10.3748/wjg.v20.i47.17985

Zhong, F., Zhou, X., Xu, J., & Gao, L. (2020). Rodent Models of Nonalcoholic Fatty Liver Disease. *Digestion*, *101*(5), 522–535. https://doi.org/10.1159/000501851